

Measurement of Bottom Quark Production in 1.8 TeV $p\bar{p}$ Collisions Using Muons from b -Quark Decays

F. Abe,¹² M. Albrow,⁶ D. Amidei,¹⁵ C. Anway-Wiese,³ G. Apollinari,²³ M. Atac,⁶ P. Auchincloss,²² P. Azzi,¹⁷ N. Bacchetta,¹⁶ A. R. Baden,⁸ W. Badgett,¹⁵ M. W. Bailey,²¹ A. Bamberger,^{6,*} P. de Barbaro,²² A. Barbaro-Galtieri,¹³ V. E. Barnes,²¹ B. A. Barnett,¹¹ G. Bauer,¹⁴ T. Baumann,⁸ F. Bedeschi,²⁰ S. Behrends,² S. Belforte,²⁰ G. Bellettini,²⁰ J. Bellinger,²⁸ D. Benjamin,²⁷ J. Benloch,¹⁴ J. Bensinger,² A. Beretvas,⁶ J. P. Berge,⁶ S. Bertolucci,⁷ K. Biery,¹⁰ S. Bhadra,⁹ M. Binkley,⁶ D. Bisello,¹⁷ R. Blair,¹ C. Blocker,² A. Bodek,²² V. Bolognesi,²⁰ A. W. Booth,⁶ C. Boswell,¹¹ G. Brandenburg,⁸ D. Brown,⁸ E. Buckley-Geer,⁶ H. S. Budd,²² G. Busetto,¹⁷ A. Byon-Wagner,⁶ K. L. Byrum,¹ C. Campagnari,⁶ M. Campbell,¹⁵ A. Caner,⁶ R. Carey,⁸ W. Carithers,¹³ D. Carlsmith,²⁸ J. T. Carroll,⁶ R. Cashmore,^{6,*} A. Castro,¹⁷ Y. Cen,¹⁸ F. Cervelli,²⁰ K. Chadwick,⁶ J. Chapman,¹⁵ G. Chiarelli,⁷ W. Chinowsky,¹³ S. Cihangir,⁶ A. G. Clark,⁶ M. Cobal,²⁰ D. Connor,¹⁸ M. Contreras,⁴ J. Cooper,⁶ M. Cordelli,⁷ D. Crane,⁶ J. D. Cunningham,² C. Day,⁶ F. DeJongh,⁶ S. Dell'Agnello,²⁰ M. Dell'Orso,²⁰ L. Demortier,²³ B. Denby,⁶ P. F. Derwent,¹⁵ T. Devlin,²⁴ D. DiBitonto,²⁵ M. Dickson,²² R. B. Drucker,¹³ A. Dunn,¹⁵ K. Einsweiler,¹³ J. E. Elias,⁶ R. Ely,¹³ S. Eno,⁴ S. Errede,⁹ A. Etchegoyen,^{6,*} B. Farhat,¹⁴ M. Frautschi,¹⁶ G. J. Feldman,⁸ B. Flaughner,⁶ G. W. Foster,⁶ M. Franklin,⁸ J. Freeman,⁶ H. Frisch,⁴ T. Fuess,⁶ Y. Fukui,¹² A. F. Garfinkel,²¹ A. Gauthier,⁹ S. Geer,⁶ D. W. Gerdes,¹⁵ P. Giannetti,²⁰ N. Giokaris,²³ P. Giromini,⁷ L. Gladney,¹⁸ M. Gold,¹⁶ J. Gonzalez,¹⁸ K. Goulios,²³ H. Grassmann,¹⁷ G. M. Grieco,²⁰ R. Grindley,¹⁰ C. Grosso-Pilcher,⁴ C. Haber,¹³ S. R. Hahn,⁶ R. Handler,²⁸ K. Hara,²⁶ B. Harral,¹⁸ R. M. Harris,⁶ S. A. Hauger,⁵ J. Hauser,³ C. Hawk,²⁴ T. Hessing,²⁵ R. Hollebeek,¹⁸ L. Holloway,⁹ A. Hölscher,¹⁰ S. Hong,¹⁵ G. Houk,¹⁸ P. Hu,¹⁹ B. Hubbard,¹³ B. T. Huffman,¹⁹ R. Hughes,²² P. Hurst,⁸ J. Huth,⁶ J. Hylen,⁶ M. Incagli,²⁰ T. Ino,²⁶ H. Iso,²⁶ H. Jensen,⁶ C. P. Jessop,⁸ R. P. Johnson,⁶ U. Joshi,⁶ R. W. Kadel,¹³ T. Kamon,²⁵ S. Kanda,²⁶ D. A. Kardelis,⁹ I. Karliner,⁹ E. Kearns,⁸ L. Keeble,²⁵ R. Kephart,⁶ P. Kesten,² R. M. Keup,⁹ H. Keutelian,⁶ D. Kim,⁶ S. B. Kim,¹⁵ S. H. Kim,²⁶ Y. K. Kim,¹³ L. Kirsch,² K. Kondo,²⁶ J. Konigsberg,⁸ K. Kordas,¹⁰ E. Kovacs,⁶ M. Krasberg,¹⁵ S. E. Kuhlmann,¹ E. Kuns,²⁴ A. T. Laasanen,²¹ S. Lammel,³ J. I. Lamoureux,²⁸ T. LeCompte,⁹ S. Leone,²⁰ J. D. Lewis,⁶ W. Li,¹ P. Limon,⁶ M. Lindgren,³ T. M. Liss,⁹ N. Lockyer,¹⁸ M. Loretì,¹⁷ E. H. Low,¹⁸ D. Lucchesi,²⁰ C. B. Luchini,⁹ P. Lukens,⁶ P. Maas,²⁸ K. Maeshima,⁶ M. Mangano,²⁰ J. P. Marriner,⁶ M. Mariotti,²⁰ R. Markeloff,²⁸ L. A. Markosky,²⁸ J. A. J. Matthews,¹⁶ R. Mattingly,² P. McIntyre,²⁵ A. Menzione,²⁰ E. Meschi,²⁰ T. Meyer,²⁵ S. Mikamo,¹² M. Miller,⁴ T. Mimashi,²⁶ S. Miscetti,⁷ M. Mishina,¹² S. Miyashita,²⁶ Y. Morita,²⁶ S. Moulding,²³ J. Mueller,²⁴ A. Mukherjee,⁶ T. Muller,³ L. F. Nakae,² I. Nakano,²⁶ C. Nelson,⁶ D. Neuberger,³ C. Newman-Holmes,⁶ J. S. T. Ng,⁸ M. Ninomiya,²⁶ L. Nodulman,¹ S. Ogawa,²⁶ R. Paoletti,²⁰ V. Papadimitriou,⁶ A. Para,⁶ E. Pare,⁸ S. Park,⁶ J. Patrick,⁶ G. Pauletta,²⁰ L. Pescara,¹⁷ T. J. Phillips,⁵ A. G. Piacentino,²⁰ R. Plunkett,⁶ L. Pondrom,²⁸ J. Proudfoot,¹ F. Ptohos,⁸ G. Punzi,²⁰ D. Quarrie,⁶ K. Ragan,¹⁰ G. Redlinger,⁴ J. Rhoades,²⁸ M. Roach,²⁷ F. Rimondi,^{6,*} L. Ristori,²⁰ W. J. Robertson,⁵ T. Rodrigo,⁶ T. Rohaly,¹⁸ A. Roodman,⁴ W. K. Sakumoto,²² A. Sansoni,⁷ R. D. Sard,⁹ A. Savoy-Navarro,⁶ V. Scarpine,⁹ P. Schlabach,⁸ E. E. Schmidt,⁶ O. Schneider,¹³ M. H. Schub,²¹ R. Schwitters,⁸ G. Sciacca,²⁰ A. Scribano,²⁰ S. Segler,⁶ S. Seidel,¹⁶ Y. Seiya,²⁶ G. Sganos,¹⁰ M. Shapiro,¹³ N. M. Shaw,²¹ M. Sheaff,²⁸ M. Shochet,⁴ J. Siegrist,¹³ A. Sill,²² P. Sinervo,¹⁰ J. Skarha,¹¹ K. Sliwa,²⁷ D. A. Smith,²⁰ F. D. Snider,¹¹ L. Song,⁶ T. Song,¹⁵ M. Spahn,¹³ P. Sphicas,¹⁴ A. Spies,¹¹ R. St. Denis,⁸ L. Stanco,¹⁷ A. Stefanini,²⁰ G. Sullivan,⁴ K. Sumorok,¹⁴ R. L. Swartz, Jr.,⁹ M. Takano,²⁶ K. Takikawa,²⁶ S. Tarem,² F. Tartarelli,²⁰ S. Tether,¹⁴ D. Theriot,⁶ M. Timko,²⁷ P. Tipton,²² S. Tkaczyk,⁶ A. Tollestrup,⁶ J. Tonnison,²¹ W. Trischuk,⁸ Y. Tsay,⁴ J. Tseng,¹¹ N. Turini,²⁰ F. Ukegawa,²⁶ D. Underwood,¹ S. Vejck III,¹⁵ R. G. Wagner,¹ R. L. Wagner,⁶ N. Wainer,⁶ R. C. Walker,²² J. Walsh,¹⁸ A. Warburton,¹⁰ G. Watts,²² T. Watts,²⁴ R. Webb,²⁵ C. Wendt,²⁸ H. Wenzel,²⁰ W. C. Wester III,¹³ T. Westhusing,⁹ S. N. White,²³ A. B. Wicklund,¹ E. Wicklund,⁶ H. H. Williams,¹⁸ B. L. Winer,²² J. Wolinski,²⁵ D. Y. Wu,¹⁵ X. Wu,²⁰ J. Wyss,¹⁷ A. Yagil,⁶ K. Yasuoka,²⁶ Y. Ye,¹⁰ G. P. Yeh,⁶ J. Yoh,⁶ M. Yokoyama,²⁶ J. C. Yun,⁶ A. Zanetti,²⁰ F. Zetti,²⁰ S. Zhang,¹⁵ W. Zhang,¹⁸ and S. Zucchelli^{6,*}

(CDF Collaboration)

¹Argonne National Laboratory, Argonne, Illinois 60439

²Brandeis University, Waltham, Massachusetts 02254

- ³University of California at Los Angeles, Los Angeles, California 90024
⁴University of Chicago, Chicago, Illinois 60637
⁵Duke University, Durham, North Carolina 27706
⁶Fermi National Accelerator Laboratory, Batavia, Illinois 60510
⁷Laboratori Nazionali di Frascati, Istituto Nazionale di Fisica Nucleare, Frascati, Italy
⁸Harvard University, Cambridge, Massachusetts 02138
⁹University of Illinois, Urbana, Illinois 61801
¹⁰Institute of Particle Physics, McGill University, Montreal, and University of Toronto, Toronto, Canada
¹¹The Johns Hopkins University, Baltimore, Maryland 21218
¹²National Laboratory for High Energy Physics (KEK), Tsukuba, Ibaraki 305, Japan
¹³Lawrence Berkeley Laboratory, Berkeley, California 94720
¹⁴Massachusetts Institute of Technology, Cambridge, Massachusetts 02139
¹⁵University of Michigan, Ann Arbor, Michigan 48109
¹⁶University of New Mexico, Albuquerque, New Mexico 87131
¹⁷Università di Padova, Istituto Nazionale di Fisica Nucleare, Sezione di Padova, I-35131 Padova, Italy
¹⁸University of Pennsylvania, Philadelphia, Pennsylvania 19104
¹⁹University of Pittsburgh, Pittsburgh, Pennsylvania 15260
²⁰Istituto Nazionale di Fisica Nucleare, University and Scuola Normale Superiore of Pisa, I-56100 Pisa, Italy
²¹Purdue University, West Lafayette, Indiana 47907
²²University of Rochester, Rochester, New York 15627
²³Rockefeller University, New York, New York 10021
²⁴Rutgers University, Piscataway, New Jersey 08854
²⁵Texas A&M University, College Station, Texas 77843
²⁶University of Tsukuba, Tsukuba, Ibaraki 305, Japan
²⁷Tufts University, Medford, Massachusetts 02155
²⁸University of Wisconsin, Madison, Wisconsin 53706
(Received 8 June 1993)

We present a measurement of the b -quark cross section in 1.8 TeV $p\bar{p}$ collisions recorded with the Collider Detector at Fermilab using muonic b -quark decays. In the central rapidity region ($|y^b| < 1.0$), the cross section is $295 \pm 21 \pm 75$ nb ($59 \pm 14 \pm 15$ nb) for $p_T^b > 21$ GeV/ c (29 GeV/ c). Comparisons are made to previous measurements and next-to-leading order QCD calculations.

PACS numbers: 13.85.Qk

The b -quark production cross section in hadron collisions is predicted by several next-to-leading order QCD calculations [1–3]. Our previous semileptonic measurement, using high p_T electrons [4], found this cross section to be 1.4 to 2.2 standard deviations higher than the theoretical calculation [2]. We report an additional measurement of this cross section for two regions of transverse momenta in $p\bar{p}$ collisions at $\sqrt{s} = 1.8$ TeV using high p_T muons from semileptonic b -quark decays. This measurement, using a separate data sample, has different sources of systematic uncertainties and is a nearly independent test of the theory. The first measurement of hadronic b -quark production based on semileptonic b -quark decays was performed by the UA1 Collaboration at $\sqrt{s} = 0.63$ TeV [5].

The data were taken in 1988–1989 using the Collider Detector at Fermilab (CDF) [6]. In the central region of pseudorapidity $|\eta| < 1$, the central tracking chamber (CTC) measures the momenta of charged particles with a resolution of $\delta p_T/p_T \approx 0.002 p_T$ (p_T in GeV/ c). The muon chamber system, covering the range $|\eta| < 0.63$, surrounds the central calorimeter which has a thickness of approximately five absorption lengths for charged pions at normal incidence.

The data sample, obtained with a multilevel trigger, corresponds to an integrated luminosity of 3.79 ± 0.26 pb $^{-1}$. The level 1 trigger required the presence of a track in the muon chambers with a p_T greater than ~ 3 GeV/ c for approximately two-thirds of the data used in this analysis and 5 GeV/ c for the other one-third. The level 2 trigger required that a track found in the muon chambers match a track reconstructed by the CTC hardware track processor within $\pm 15^\circ$ in azimuth and have p_T greater than ~ 9 GeV/ c . The software level 3 trigger required the track to have p_T greater than 11 GeV/ c . The data were divided into two bins in muon candidate p_T . For the lower bin ($12 < p_T < 17$ GeV/ c), the combined efficiency of the level 1, 2, and 3 triggers (ϵ_{trig}) was 0.88 ± 0.02 , and for the upper bin ($17 < p_T < 22$ GeV/ c), it was 0.91 ± 0.02 [7].

A number of additional cuts were applied in order to insure the reliability of the track fits and to reject background. The z position of the event vertex was required to be within ± 60 cm of the detector center. The CTC tracks were required to intersect the muon chambers at least 10 cm from their edges in z , to pass within 10 cm of the event vertex in z , and have an impact parameter (in the transverse plane) of less than 0.15 cm. The match of

the muon chamber track and the associated CTC track was required to be compatible with the deviation expected from multiple scattering in the material traversed by the muon. The efficiency for each of these cuts was measured independently using muons from cosmic ray data, J/ψ decay, and W and Z boson decay. The weighted average of the individual cut efficiencies determined in each of these samples was used. The product of the above cut efficiencies was $0.820 \pm 0.031 \pm 0.010$ ($0.850 \pm 0.025 \pm 0.010$) for the lower (upper) p_T bin, where the first error is statistical and the second systematic. Finally, in order to reject events in which hadrons showering in the calorimeter satisfied the above cuts, candidate muons were rejected if the energy registered in the hadron calorimeter towers they traversed was greater than 5 GeV. This compares with 2 GeV for an isolated muon. The efficiency of this hadron energy cut was determined using a Monte Carlo simulation which included ISAJET [8] for b -quark production, the Peterson model with $\epsilon=0.006$ for b fragmentation [9], the CLEO Monte Carlo simulation for the B decay [10], and a complete detector simulation. This efficiency is $0.910 \pm 0.003 \pm 0.022$ ($0.856 \pm 0.006 \pm 0.013$) for b -quark muons in the lower (upper) p_T bin. The assigned systematic errors reflect uncertainties in the production model and in the b fragmentation function. Combining this result with the previous cut efficiency, the total analysis cut efficiency (ϵ_{cut}) is $0.746 \pm 0.028 \pm 0.022$ ($0.728 \pm 0.022 \pm 0.018$) for the lower (upper) p_T bin.

The principal backgrounds to heavy quark muonic decays are punchthrough hadrons and muons from π and K decays in flight. Other backgrounds include single muons from W decay and cosmic rays, and dimuons from Z decay and the Drell-Yan process. Punchthrough hadrons, the largest background, are hadrons which penetrate the calorimeters without showering and hence cannot be distinguished from muons on a track-by-track basis. To remove this background, we took advantage of the difference between the η distributions of real muons and punchthrough hadrons. Prompt and decay-in-flight muons have a nearly flat η distribution, while that of punchthrough hadrons falls with η as the calorimeter thickness increases. We fitted the data η distribution, corrected for geometrical acceptance and the vertex z distribution, to the sum of these two distributions.

Using the Monte Carlo simulation, the η distribution of muons from b -quark decays was found to be proportional to $1 - 0.173|\eta|$ for $|\eta| < 0.72$. Although the prompt muons from charm decays and muons from decay in flight are even flatter in η , the same form was used to represent all three muon sources and a systematic error was assigned to account for the differences. The punchthrough hadron η distribution was represented by the form $\sum_i A_i \exp(-\Lambda_i/\sin\theta)$, where A_i represents the fraction of the i th hadron produced ($i=K^+, K^-, \pi^+, \pi^-, p, \bar{p}$) and Λ_i is the calorimeter thickness in absorption lengths at normal incidence. The hadron production frac-

tions at the Fermilab Tevatron are known only for moderate p_T [11]. We estimated these fractions for $p_T > 12$ GeV/c to be $K/\pi=0.28$ and $(p+\bar{p})/\pi=0.04$ [12].

Figure 1(a) [1(b)] shows the fit of the muon and punchthrough hadron η distributions to the acceptance corrected η distribution found in the data for the lower (upper) p_T bin. The dashed curves show the distributions associated with real muons and punchthrough hadrons. From this fit, we obtained a muon fraction $f_\mu=0.55 \pm 0.01$ (0.47 ± 0.04) based on 14667 (2418) events.

The systematic uncertainties of the fit were determined by varying the input parameters independently and refitting the distributions. The K/π ratio was varied from 0.10 to 0.33, the $(p+\bar{p})/\pi$ ratio was varied by $\pm 100\%$, and the slope of the line representing the muon distribution was varied by $\pm 12\%$. The K^+ absorption length, which is the longest and the one to which we are most sensitive, was varied by $\pm 5\%$ [13]. The effect of including the flatter decay-in-flight η distribution with the prompt muon distribution was estimated by fitting with an additional constant term. The overall differences between the adjusted and nominal fits resulted in a systematic uncertainty equal to $\pm 6\%$ of the b -quark cross section.

Muons from pion and kaon decay in flight constitute another significant background. The number of muons from decay in flight was determined using the inclusive single charged particle $d\sigma/dp_T$ distribution [12] obtained from CDF minimum bias data [14] and supplemented in the range $6 < p_T < 20$ GeV/c by a data sample obtained

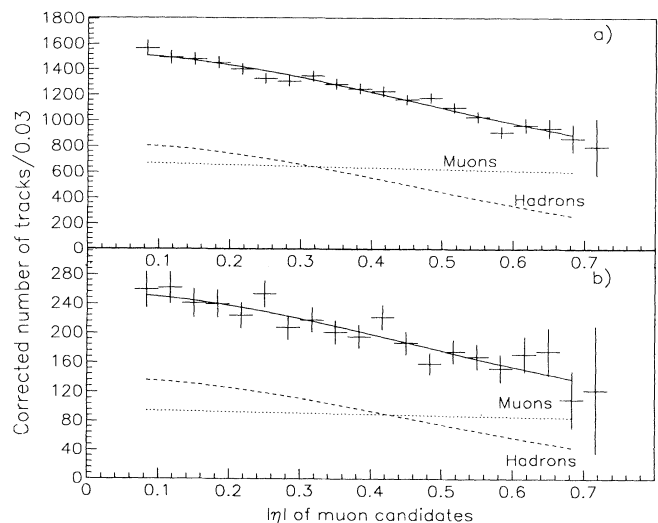


FIG. 1. The result of fitting the acceptance corrected η distribution of the muon candidates to muon and punchthrough hadron components, (a) $12 < p_T < 17$ GeV/c, (b) $17 < p_T < 22$ GeV/c. The dashed curves show the fitted muon and punchthrough hadron components while the solid curve is their sum.

using a high p_T single-track trigger. This distribution was extrapolated beyond 20 GeV/c by using a sample of jets with transverse energy $E_T > 20$ GeV [12]. Pions and kaons were generated according to this distribution and decayed and tracked through the detector using the simulation. The muon selection cuts described above were then applied. Using the rate of simulated decay-in-flight muons passing the analysis cuts and folding in the detector acceptance and the integrated luminosity, the number of decay-in-flight muons in our sample was estimated (Table I). The systematic uncertainty on the number of decay-in-flight muons was dominated by the uncertainty in the tracking efficiency ($\pm 4\%$) and the K/π ratio ($\pm 3\%$).

Background muons from W decay were eliminated if they had both missing $E_T > 20$ GeV and transverse mass greater than 20 GeV/c². Z decays to muon pairs were removed if their invariant mass was greater than 65 GeV/c². Residual W and Z backgrounds were determined from Monte Carlo studies. The Drell-Yan background was calculated [15], and the cosmic ray background estimated [12]. The sum of these backgrounds is shown in Table I under N_{bkg} .

Finally, a correction was made for the contribution from charm quark decays to muons. If b and c quarks were produced at the same rate at high p_T , the fact that muons from b decays have a much harder spectrum due to their harder fragmentation function and higher Q value would lead to an estimated charm to bottom ratio (c/b) in our sample of ~ 0.15 . We attempted to measure c/b directly by studying the component of the muon momentum perpendicular to the jet axis, which is sensitive to the mass of the parent hadron [5]. Because of the large background, it was only possible to set an upper limit on c/b of 0.36 at 90% C.L. The result of a next-to-leading order calculation by Nason, Dawson, and Ellis

TABLE I. The total number of muon candidates after cuts (N_{tot}), the fraction of muons (f_μ), the calculated number of decay-in-flight muons ($\sigma_{\text{DIF}}L_{\text{int}}$), the estimated number of remaining background events (N_{bkg}), and the total number of prompt muons are all quantities used in Eq. (1) to calculate the cross section in $|\eta| < 1.0$ of muons from b -quark decays (σ_μ). The corresponding b -quark cross section for $p_T^b > p_T^{\text{min}}$ and $|\eta| < 1.0$ is $\sigma_b(p_T^{\text{min}})$.

Muon p_T^b	12–17 GeV/c	17–22 GeV/c
N_{tot}	14667	2418
f_μ	$0.55 \pm 0.01 \pm 0.028$	$0.47 \pm 0.04 \pm 0.027$
$\sigma_{\text{DIF}}L_{\text{int}}$	$3425 \pm 193 \pm 205$	$492 \pm 110 \pm 31$
N_{bkg}	148 ± 37	35 ± 8
No. prompt μ	$4674 \pm 243 \pm 460$	$609 \pm 147 \pm 73$
σ_μ (nb)	$3.60 \pm 0.25 \pm 0.57$	$0.50 \pm 0.12 \pm 0.08$
p_T^{min}	21 GeV/c	29 GeV/c
$\sigma_b(p_T^{\text{min}})$ (nb)	$295 \pm 21 \pm 75$	$59 \pm 14 \pm 15$

(NDE) [2] with MRSD0 [16] structure function and $\mu^2 = 4(p_T^2 + m_b^2)$ is that the c to b quark production ratio is 1.4 and 1.2 for $p_T^{b,c} > 21$ and $p_T^{b,c} > 29$ GeV/c, respectively. We used this result and estimated the charm to bottom ratio in our sample, after all cuts, to be $c/b = 0.24 \pm 0.12$ (0.16 ± 0.08) in the lower (upper) p_T bin. These errors correspond to a $\pm 50\%$ variation in the production ratio and results in a $\pm 9.8\%$ systematic uncertainty on the b cross section.

The following expression was used to calculate the cross section for muons from b -quark decays:

$$\sigma_\mu = \frac{N_{\text{tot}}f_\mu - \sigma_{\text{DIF}}L_{\text{int}} - N_{\text{bkg}}}{\epsilon_{\text{trig}}\epsilon_{\text{cut}}\epsilon_{\text{acc}}L_{\text{int}}} \left(\frac{b}{b+c} \right), \quad (1)$$

where ($N_{\text{tot}}f_\mu$) is the total number of muons obtained from the fit to the η distribution, $\sigma_{\text{DIF}}L_{\text{int}}$ is the calculated number of muons from π and K decay in flight, and N_{bkg} is the remaining number of background muons excluding charm decays. The $b \rightarrow \mu X$ acceptance in the angular region $|\eta| < 1$, was determined to be $\epsilon_{\text{acc}} = 0.421 \pm 0.002 \pm 0.011$. The trigger efficiency (ϵ_{trig}), the p_T dependent total analysis cut efficiency (ϵ_{cut}), the integrated luminosity (L_{int}), and the b fraction $b/(b+c)$ have been discussed above. Table I shows the result [12].

To calculate the b -quark production cross section we used the following equation:

$$\sigma_b(p_T^{\text{min}}) = \frac{1}{2} \sigma_\mu \frac{\sigma_{\text{MC}}(p_T^b > p_T^{\text{min}})}{\sigma_{\text{MC}}(\text{per } p_T^b \text{ bin})}, \quad (2)$$

where σ_μ [from Eq. (1)] is the measured cross section for muons from b decays, and p_T^{min} is the b -quark transverse momentum for which 90% of the events in a given muon p_T bin come from b quarks with $p_T > p_T^{\text{min}}$. The ratio of the b -quark production cross section for momenta above p_T^{min} and $|\eta| < 1.0$ to the cross section for producing b quarks which decay to muons in the corresponding p_T^b bin and $|\eta| < 1.0$ was obtained from the Monte Carlo simulation. We find $p_T^{\text{min}} = 21$ and 29 GeV/c for the p_T^b bins of 12–17 GeV/c and 17–22 GeV/c, respectively. The Monte Carlo simulation reproduced the shape of the NDE b -quark p_T distribution, and the uncertainties in this shape and in the fragmentation function contribute $\pm 12\%$ and $\pm 15\%$, respectively, to the systematic uncertainty in the b -quark cross section. The leading factor of $\frac{1}{2}$ is necessary to obtain the b -quark cross section, not including \bar{b} . The resulting cross sections are shown in Table I.

Figure 2 shows the measured b -quark cross sections compared to the next-to-leading order NDE calculation, with auxiliary curves indicating the theoretical uncertainty arising from the uncertainty in their choice of renormalization scale μ , b -quark mass, and QCD parameter Λ . Figure 2 also shows results from other CDF measurements using $B^\pm \rightarrow J/\psi K^\pm$ and $B^0 \rightarrow J/\psi K^*$ [17], and inclusive $\psi(2S)$, J/ψ [18], and electron events [4]. For $p_T^b > 21$ GeV/c a discrepancy of 2.1 standard deviations is observed between our measurement and the central

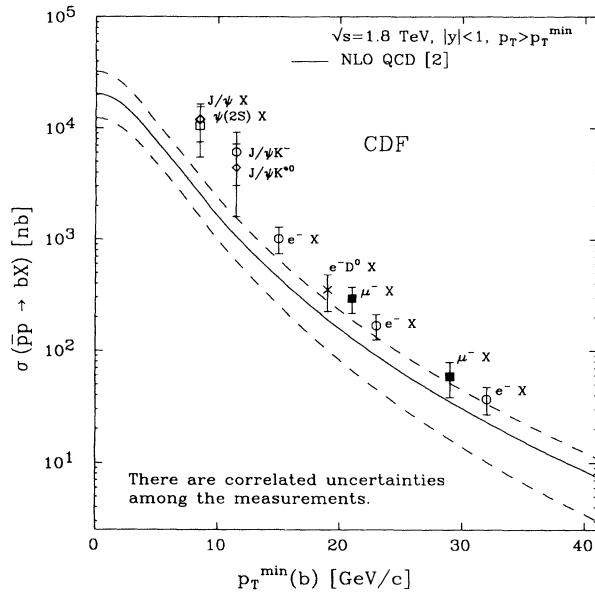


FIG. 2. Cross section for the production of b quarks with $p_T^b > p_T^{\min}$ from inclusive muon decays (this analysis shaded) with statistical and systematic uncertainties added in quadrature. Previous measurements [4,17,18] are also shown. The solid line is a next-to-leading order calculation of Nason, Dawson, and Ellis [2], while the dashed curve resulted from varying parameters in the calculation.

theoretical value, while for $p_T^b > 29$ GeV/c they are in agreement within the experimental errors. This result supports the conclusion of previous CDF analyses that the next-to-leading order QCD calculation tends to underestimate the inclusive b -quark cross section.

We thank the Fermilab staff and the technical staffs of the participating institutions for their vital contributions. This work was supported by the U.S. Department of Energy and National Science Foundation, the Italian Istituto Nazionale di Fisica Nucleare, the Ministry of Science,

Culture, and Education of Japan, and the A.P. Sloan Foundation.

*Visitor.

- [1] P. Nason, S. Dawson, and R. K. Ellis, Nucl. Phys. **B303**, 607 (1988); G. Altarelli, M. Diemoz, G. Martinelli, and P. Nason, Nucl. Phys. **B308**, 724 (1988).
- [2] P. Nason, S. Dawson, and R. K. Ellis, Nucl. Phys. **B327**, 49 (1989).
- [3] W. Beenakker, H. Kuijff, W. L. van Neeven, and J. Smith, Phys. Rev. D **40**, 54 (1989).
- [4] F. Abe *et al.*, Report No. FERMILAB-PUB-93/091-E (to be published).
- [5] C. Albajar *et al.*, Phys. Lett. B **186**, 237 (1987); **213**, 405 (1988); **256**, 121 (1991).
- [6] F. Abe *et al.*, Nucl. Instrum. Methods Phys. Res., Sect. A **271**, 387 (1988), and references therein.
- [7] F. Abe *et al.*, Phys. Rev. D **43**, 2070 (1991).
- [8] F. Paige and S. D. Protopopescu, BNL Report No. BNL383034, 1986 (unpublished). We used version 6.43.
- [9] C. Peterson *et al.*, Phys. Rev. D **27**, 105 (1983); J. Chrin, Z. Phys. C **36**, 163 (1987).
- [10] The Monte Carlo program is tuned to the results from S. Henderson *et al.*, Phys. Rev. D **45**, 2212 (1992), who measured the semileptonic branching fraction of B mesons to muons to be $(11.2 \pm 0.6)\%$.
- [11] T. Alexopoulos *et al.*, Report No. UNDHEP 93-05 (to be published).
- [12] B. Todd Huffman, Ph.D. thesis, Purdue University, 1992.
- [13] S. P. Denisov *et al.*, Nucl. Phys. **B61**, 62 (1973).
- [14] F. Abe *et al.*, Phys. Rev. Lett. **61**, 1819 (1988).
- [15] F. Abe *et al.*, Phys. Rev. Lett. **67**, 2418 (1991).
- [16] A. D. Martin, W. J. Stirling, and R. G. Roberts, Phys. Rev. D **47**, 867 (1993).
- [17] F. Abe *et al.*, Phys. Rev. Lett. **68**, 3403 (1992); F. Abe *et al.*, Report No. FERMILAB-PUB-93/131-E (to be published).
- [18] F. Abe *et al.*, Phys. Rev. Lett. **69**, 3704 (1992); F. Abe *et al.*, Report No. FERMILAB-PUB-93/106-E (to be published). These papers assume no direct J/ψ or $\psi(2S)$ production.